ICAS 2020 SHANGHAI
International Council of the Aeronautical Sciences
32nd Congress of the International Council of the Aeronautical Sciences
Shanghai, China
September 14th-18th, 2020

AIRCRAFT INFLIGHT ICING DETECTION AND DIAGNOSIS METHODS

Di Ding[1,2], Wei-Qi Qian[1] & Qing Wang[1]

[1]Computational Aerodynamics Institute, China Aerodynamics Research and Development Center, Mianyang 621000, China
[2]State Key Laboratory of Aerodynamics, China Aerodynamics Research and Development Center, Mianyang 621000, China

Abstract

Aircraft inflight icing is one of the most serious threats to flight safety. Although the devices of detectors and sensors for ice probing is widely used, there still has a strong demand to develop mathematical detection algorithms as an auxiliary means for the insufficient or incapable usage of the devices. This paper focuses on the issue of aircraft inflight icing detection by algorithms. First the icing research airbus and the aircraft dynamic model with wing ice are introduced. Second the time-varying parameter identification method and the statistical diagnosis method are presented and evaluated respectively by the simulation data of a steady-level flight scenario with wing ice. Based on the conclusion of the research, the diagnosis residual, window size and identification parameters are chosen. Last a scheme of combining the two methods for aircraft inflight icing detection is proposed. The same flight scenario is utilized to assess the effectiveness of the detection strategy. The results show the icing alarm and the changing information of aerodynamic parameters all can be detected by the scheme. The stability derivatives can be identified from the excited output in a relatively high accuracy with the help of superposing a small disturbance signal to the input after the icing alarm. The results of the strategy indicate the feasibility of applying the combining algorithm in real flight tests.

Keywords: aircraft ice detection, aerodynamic parameter identification, statistical diagnosis, H_∞ filter, GLRT method

1. Introduction

Aircraft inflight icing is one of the most severe threats to flight safety, sometimes it even leads to fatal accidents and casualties. Based on statistic data given by the American Safety Advisor, from 1990 to 2000, there are 12% of all the flight accidents which resulted from adverse weather conditions that occurred in icing and 92% of the ice induced accidents that took place in inflight icing [1]. Thus, the icing detection and protection technologies become more and more important in the aviation industry. The ice protection system usually needs the ice alarm signal to actuate the de-ice or anti-ice devices. There are two main means to detect the alarm signal: the direct detection using detectors or sensors [2-3], and the indirect detection using mathematical algorithms. Although many aircrafts have utilized the direct detection technology successfully, there still is a strong demand to develop detection algorithms as an auxiliary means for the insufficient or incapable usage of the direct detection method. Since the concept of Smart Icing System [4] presented by NASA icing research group, the studies on indirect detection methods have been developed rapidly. There are three main types of algorithms for aircraft inflight icing detection: the parameter identification method, the data-based modelling method, and the observer-based detection method. The parameter identification method estimates the flight status and the changing aerodynamic parameters jointly by filtering algorithms, such as Extended Kalman Filter (EKF) [5-6], H∞ filter [6-8] and Multiple Model Adaptive Estimator (MMAE) [9-10]. The parameterized ice accretion process can be estimated by these filters or estimators, then the changing information of the ice influenced parameter can be used for reconfiguring the flight control

law [11-13] and maintaining the aircraft stability in icing conditions. The data-based modelling method models the correlations between the aircraft flight status and the ice information, including ice influenced parameters, icing severity factor, position and time, etc. Caliskan [13] designed a Neural Network (NN) to identify the ice influenced parameters from the measured data, Schuchard [14] also developed an artificial NN method to detect the presence of ice and classify its severity, Dong [15-16] utilized a probabilistic NN to decide the ice location. For ice detection, data-based modelling methods can obtain as many icing details as parameter identification methods, but the problems of the two approaches, like the over-fitting and generalization problems of data-based modelling methods and the parameter identifiability and accuracy problems of identification methods, limit the usages of the two methods in some circumstances. The observer-based detection method is more effective in giving an icing alarm. There are two applications of this method: the model-based fault diagnosis technique and the statistical diagnosis technique. The model-based fault diagnosis technique models the aircraft failure (including actuator [17], sensor [18], structure and icing [19-21]) and then detects this failure by estimators. The statistical diagnosis technique uses hypothesis testing theory to detect the changes in the observed flight data. This diagnosis approach does not require a priori statistical characteristics of the faults and has low computational cost. The innovation approach [12,22-23] and the Neyman Pearson based statistical change detection approach [24] are the commonly used statistical diagnosis techniques for aircraft icing detection, the former one directly uses the hypothesis testing on the innovation sequence to determine the changes of the aircraft flight status, its performance relies on the predetermined confidence coefficient. While the NP based diagnosis technique has a predictable performance under the NP theory, and is proved to be the optimal test subject to a constant probability of false alarm. However, the statistical diagnosis method can only be acting as the ice alarm and cannot be able to track the ice accretion information as other two methods.

This paper focuses on the issue of developing the effective aircraft inflight icing detection method. The H_∞ parameter identification method and the NP based statistical diagnosis method are discussed and assessed. The researches validate the parameter change tracking capability of the identification method and the alarm trigger capability of the statistical diagnosis method. Then a strategy of combining the two methods is proposed to remedy their own defects. The parameter identifiability and accuracy problem of the identification method and the insufficient information acquisition problem of the diagnosis method all can be resolved by this strategy. The results indicate this integrated algorithm is an effective and feasible strategy for aircraft inflight icing detection.

2. Aircraft inflight icing dynamics model

2.1 Icing Research Airbus

An airbus model is specifically presented for the aircraft icing research by the research group. The prototype has the similar aerodynamic and flight dynamic characteristics as Boeing 737 and Airbus A320. Figure 1 shows the configuration structure of the airbus, and Table 1 lists its physical parameters.

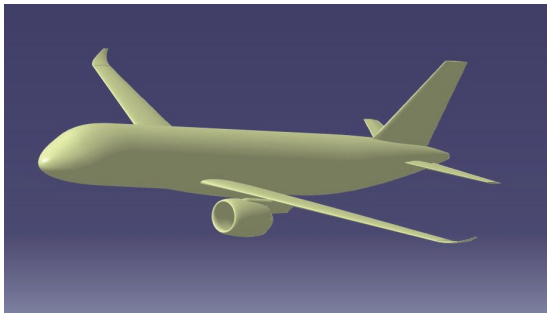

Figure 1 – Icing research airbus 3D structure.

Table 1 – Parameters of icing research airbus.

Aircraft Parameters	Values
Mass m	72000 kg
Wing reference area S	124 m^2
Wing span l	34.1 m
Mean aerodynamic chord b_A	4.15 m
Moment of inertia I_{xx}	1658755 kg×m^2
Moment of inertia I_{yy}	2392630 kg×m^2
Moment of inertia I_{zz}	3846326 kg×m^2

2.2 Aerodynamic Characteristics of Airbus

The aerodynamic characteristics of the airbus is calculated by computational fluid dynamics (CFD) tool. RANS and multi-block structured grid are used to obtain the longitudinal aerodynamic characteristics with clean and severe wing ice configuration (Figure 2). Then a polynomial equation (1) is used to fit the longitudinal characteristics, where C_D, C_L, and C_M represent drag, lift and pitch moment coefficients respectively, α is the angle of attack (AOA), q is the pitch rate, δ_e is the elevator angle. The aircraft's stability and control derivatives in two configurations are compared in Table 2. Because the influence of wing ice on C_{D0}, C_{L0}, and C_{M0} is relatively small, here only the derivatives that are more affected by wing ice are fitted in this table. The results indicate wing icing increases drag derivatives, and decreases lift, pitch moment derivatives and control surface efficiency.

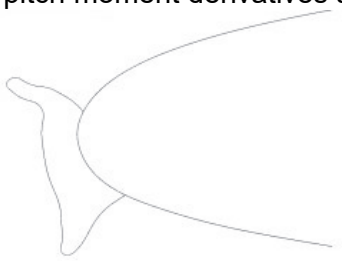

Figure 2 – Severe wing ice.

$$\begin{aligned} C_D &= C_{D0} + C_{D\alpha}\alpha \\ C_L &= C_{L0} + C_{L\alpha}\alpha + C_{L\delta e}\delta_e \\ C_M &= C_{M0} + C_{M\alpha}\alpha + C_{M\dot{\alpha}}\dot{\alpha} + C_{Mq}q + C_{M\delta e}\delta_e \end{aligned} \tag{1}$$

Table 2 – Longitudinal derivatives of icing research airbus in clean and severe iced configurations.

Longitudinal Derivatives	Clean	Severe Iced
C_{D0}	0.0277	0.0277
$C_{D\alpha}$	0.1069	0.7701
$C_{D\delta e}$	0	0.0149
C_{L0}	0.1415	0.1415
$C_{L\alpha}$	6.2326	3.0637
$C_{L\delta e}$	0.448	0.2848
C_{M0}	0.0353	0.0353
$C_{M\alpha}$	-1.7873	-1.2762
$C_{M\dot{\alpha}}$	-13.7477	-13.0491
C_{Mq}	-41.513	-39.4878
$C_{M\delta e}$	-1.9035	-1.3476

2.3 Aircraft icing flight dynamics model

The longitudinal flight dynamics considering ice accretion process for aircraft is modelled. The motion and rotation equations (2) are established in the velocity and the body coordinate respectively.

$$\begin{aligned}
\dot{V} &= -\frac{q_\infty S}{m} C_D + \frac{P_x}{m} + g_x \\
\dot{\alpha} &= -\frac{q_\infty S}{mV\cos\beta} C_L + \frac{P_z}{mV\cos\beta} + \frac{g_z}{V\cos\beta} - \\
&\quad \frac{1}{\cos\beta}\left(p\cos\alpha\sin\beta - q\cos\beta + r\sin\alpha\sin\beta\right) \\
\dot{q} &= \frac{q_\infty S b_A}{I_{yy}} C_M + \frac{M_y}{I_{yy}} + \frac{I_{zz} - I_{xx}}{I_{yy}} pr - \frac{I_{xz}}{I_{yy}}\left(p^2 - r^2\right) \\
\dot{\theta} &= q\cos\phi - r\sin\phi \\
\dot{h} &= V\cos\alpha\cos\beta\sin\theta - V\sin\beta\cos\theta\sin\phi - \\
&\quad V\sin\alpha\cos\beta\cos\theta\cos\phi
\end{aligned} \tag{2}$$

where V is the aircraft velocity, β is the angle of sideslip, p, q, and r represents roll, pitch and yaw rates respectively, θ is pitch angle, ϕ is roll angle, h is aircraft height, q_∞ is dynamic pressure, S is wing reference area, b_A is the mean aerodynamic chord, m is the aircraft mass, P_x and P_z represent engine thrusts, M_y is the thrust moment, g_x and g_z are the gravitational acceleration components.

The change of drag, lift and pitch moment coefficients during ice accretion process needs to be modelled for analyzing the icing influence on aircraft flight dynamics. Bragg [4] of Illinois University presented a mathematical model to describe the icing influence on aerodynamic derivatives. It has already been utilized in the development of Ice Management System (IMS) and aircraft icing online detection [7,9,16]. This model is not an accurate icing influence model, but it can indicate the variation trend of the aerodynamic derivatives during ice accretion. The ice influence on aerodynamic derivatives can be expressed by:

$$C_*^{\text{iced}} = C_*^{\text{clean}}\left(1 + K_{C_*}\eta_{\text{ice}}\right) \tag{3}$$

C_* represents arbitrary aerodynamic derivative, the superscript “iced” indicates the iced derivative, and “clean” indicates the clean derivative. K_{C_*} represents the coefficient slope which depends on the modified parameter. η_{ice} is the icing severity factor, with η_{ice}=0 denoting a clean configuration, and η_{ice}=1 denoting wing iced configuration. The curve of η_{ice} represents the ice influence on aerodynamic derivative. Melody [7] gave a continuous accretion model of ice over time. The ice accretion rate is considered as a function of both atmospheric conditions and the amount of ice already accreted. The differential equation is given by:

$$\dot{\eta}_{\text{ice}} = N_1\left(1 + N_2\eta_{\text{ice}}\right)d_\eta \tag{4}$$

$$d_\eta(t) = \frac{1}{2}\left[1 - \cos\left(\frac{2\pi t}{T_{\text{cld}}}\right)\right] \tag{5}$$

$$\begin{aligned}
N_1 &= \frac{2}{N_2 T_{\text{cld}}}\ln\left[1 + N_2\eta_{\text{ice}}\left(T_{\text{cld}}\right)\right] \\
N_2 &= \frac{\eta_{\text{ice}}\left(T_{\text{cld}}\right) - 2\eta_{\text{ice}}\left(T_{\text{cld}}/2\right)}{\eta_{\text{ice}}^2\left(T_{\text{cld}}/2\right)}
\end{aligned} \tag{6}$$

T_{cld} is the ice accretion time. When T_{cld}, $\eta_{\text{ice}}(T_{\text{cld}}/2)$ and $\eta_{\text{ice}}(T_{\text{cld}})$ are given, the curve of arbitrary aerodynamic derivative varying over time can be described by equations (3)~(6). The parameters of $\eta_{\text{ice}}(T_{\text{cld}}/2)$ and $\eta_{\text{ice}}(T_{\text{cld}})$ denote the different ice accretion rates.

3. Time-Varying Aerodynamic Parameter Identification method

3.1 H∞ Filter

The dynamic model can be parameterized as:

$$\begin{aligned} \dot{\boldsymbol{x}} &= \boldsymbol{A}(\boldsymbol{y},\boldsymbol{u})\boldsymbol{\chi} + \boldsymbol{b}(\boldsymbol{y},\boldsymbol{u}) + \boldsymbol{d}_p \\ \boldsymbol{y} &= \boldsymbol{x} + \boldsymbol{d}_m \end{aligned} \tag{7}$$

where x is the system state, χ is the system unknown parameters, y is the system output, u is the input, d_p and d_m represent the process and measurement noises respectively. The time-varying parameters are formulated by a linear model

$$\dot{\boldsymbol{\chi}} = \boldsymbol{H}\boldsymbol{\chi} + \boldsymbol{K}\boldsymbol{d}_{\chi}, \quad \boldsymbol{\chi}(0) = \boldsymbol{\chi}_0 \tag{8}$$

where d_χ represents uncertainty in the parameters. H and K are the matrixes related to unknown parameters and uncertainty. χ_0 denotes the aerodynamic derivatives in clean configuration, χ denotes the derivatives with wing ice. Considering the aircraft inflight icing model (3) is driftless, which means the inherent dynamic parameter χ does not enter the evolution differentials in (8), hence $H \doteq 0$. Assuming the unknown terms of d_η and d_χ are equivalent, then the uncertainty weight K is given by

$$\boldsymbol{K} = \boldsymbol{\chi}_0 K_{C_*} N_1 \tag{9}$$

Based on the identification algorithm developed by Didinsky et al [25], the H_∞ time-varying parameter estimation algorithm for the wing ice problem is

$$\begin{aligned} \begin{bmatrix} \dot{\hat{\boldsymbol{x}}} \\ \dot{\hat{\boldsymbol{\chi}}} \end{bmatrix} &= \begin{bmatrix} 0 & \boldsymbol{A}(\boldsymbol{y},\boldsymbol{u}) \\ 0 & \boldsymbol{H} \end{bmatrix} \begin{bmatrix} \hat{\boldsymbol{x}} \\ \hat{\boldsymbol{\chi}} \end{bmatrix} + \begin{bmatrix} \boldsymbol{b} \\ 0 \end{bmatrix} + \boldsymbol{\Sigma}^{-1} \begin{bmatrix} I \\ 0 \end{bmatrix} (\boldsymbol{y} - \hat{\boldsymbol{x}}) \\ \dot{\boldsymbol{\Sigma}} &= -\boldsymbol{\Sigma} \begin{bmatrix} 0 & \boldsymbol{A}(\boldsymbol{y},\boldsymbol{u}) \\ 0 & \boldsymbol{H} \end{bmatrix} - \begin{bmatrix} 0 & 0 \\ \boldsymbol{A}(\boldsymbol{y},\boldsymbol{u})^T & \boldsymbol{H}^T \end{bmatrix} \boldsymbol{\Sigma} + \begin{bmatrix} I & 0 \\ 0 & -\gamma^{-2}\boldsymbol{Q}(\boldsymbol{y},\boldsymbol{u}) \end{bmatrix} - \boldsymbol{\Sigma} \begin{bmatrix} I & 0 \\ 0 & \boldsymbol{K}\boldsymbol{K}^T \end{bmatrix} \boldsymbol{\Sigma} \end{aligned} \tag{10}$$

where the initial conditions are $\hat{\boldsymbol{\chi}}(0) = \hat{\boldsymbol{\chi}}_0$, $\boldsymbol{\Sigma}(0) = diag(\boldsymbol{P}_0, \boldsymbol{Q}_0)$. If we use the partition of $\boldsymbol{\Sigma}$

$$\boldsymbol{\Sigma} = \begin{bmatrix} \boldsymbol{\Sigma}_1 & \boldsymbol{\Sigma}_2 \\ \boldsymbol{\Sigma}_2^T & \boldsymbol{\Sigma}_3 \end{bmatrix}$$

Then $\gamma^* \equiv 1$ could be achieved by specifying $\boldsymbol{P}_0 = \boldsymbol{I}$ and $\boldsymbol{Q} = \boldsymbol{\Sigma}_2^T \boldsymbol{\Sigma}_1^{-2} \boldsymbol{\Sigma}_2$ for any $\boldsymbol{Q}_0 > 0$.

3.2 Algorithm Performance Assessment

A steady-level cruise scenario with ice accreting on the leading edge of wings is studied to analyze the algorithm's performance. Assuming the aircraft maintains a steady-level cruise on the trimmed status, the engine thrusts are used to keep the aircraft stable in the absence of a control system. The trimmed flight status of this scenario is shown in Table 3. The measurement noise is considered and assumed to be white Gaussian noise. Its standard deviation is listed in Table 4 by referring to the measurement noises of A340 [12]. The wing ice occurs at the beginning time, the accretion time is 200s, the accretion rates are $\eta_{ice}(T_{cld})$=1.0 and $\eta_{ice}(T_{cld}/2)$=0.7 respectively. A sinusoidal disturbance signal is added to the trimmed elevator angle with amplitude of 3° and period of 40s to improve the estimation accuracy.

Table 3 – Trimmed flight status of steady-level cruise.

Flight States	Values
Height H	5000 m
Velocity V	0.3 Ma
Trimmed elevator angle δ_e	1.06 deg
Angle of attack α	0 deg
Pitch angle θ	0 deg
Pitch rate q	0 deg/s

Table 4 – Standard deviations of measurement noises.

Standard Deviation	σ_V	σ_α	σ_q	σ_θ	σ_h
Values	0.8464m/s	0.0056°	0.0069°/s	0.0289°	1m

Then the dynamic behavior of this scenario is simulated. Based on the flight data, H∞ algorithm is utilized to estimate the three stability derivatives which are mainly influenced by wing ice. The algorithm performance for this wing ice problem is assessed by analyzing the estimation results. Figure 3 gives the estimation results and the real values of $C_{D\alpha}$、$C_{L\alpha}$ and $C_{M\alpha}$. The results show the estimation results of $C_{L\alpha}$ and $C_{M\alpha}$ are smoother than $C_{D\alpha}$, this consequence is related to the poor resistance capability to noise or disturbance for estimating the axial aerodynamic parameter. The estimation results all converge to their real values after the ice accretion process ended. In the accretion process, the estimation results have some time delays to the real values. We find the time delay of $C_{D\alpha}$ is bigger than the other two derivatives, and the time delay of $C_{L\alpha}$ is the smallest.

Three indicators are defined to quantitatively assess the accuracy of H∞ algorithm, including root mean square error (RMSE), maximum absolute error (MAE) and time delays of a given icing severity factor. The comparability of these data is guaranteed by transforming the aerodynamic derivatives to their icing severity factors through equation (3). Errors and time delays are all based on the real values, and we use the smoothed results to calculate the time delays. The errors and time delays of the three stability derivatives are given in Table 5. The data show the estimation accuracy of $C_{L\alpha}$ is the highest, the accuracy of $C_{M\alpha}$ is lower than $C_{L\alpha}$ but higher than $C_{D\alpha}$. The RMSE of the three derivatives are all relatively small, even the RMSE of the most inaccurate derivative $C_{D\alpha}$ is only about 11%, while the most accurate parameter $C_{L\alpha}$ is about 1.4%. The time delays of the three derivatives are different, the delay of $C_{D\alpha}$ is about 20s, the delay of $C_{M\alpha}$ is below 10s, and the delay of $C_{L\alpha}$ is below 3s.

The results in the figure and table indicate the H∞ algorithm is suitable for identifying the time-varying aerodynamic parameters with wing ice. The icing detection based on $C_{L\alpha}$ has relatively high accuracy and low time delay.

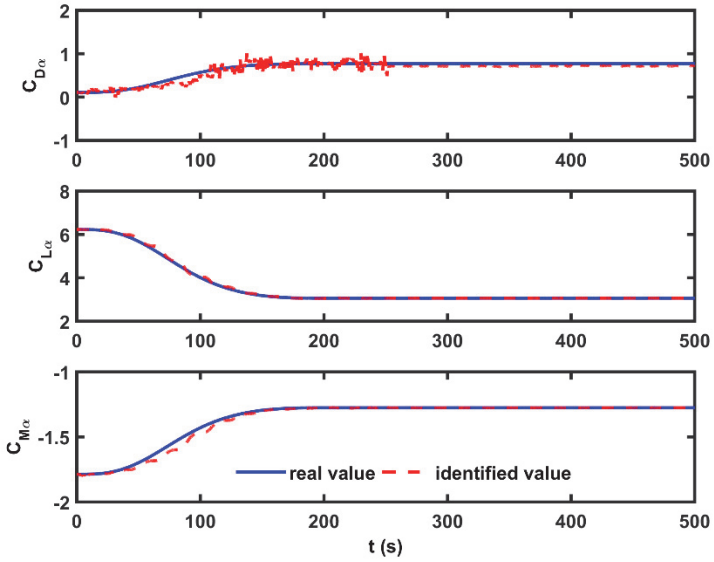

Figure 3 – Comparison of aerodynamic stability derivates results using H∞ method.

Table 5 – Error and time delay of identification results.

Errors and Delay		$C_{D\alpha}$	$C_{L\alpha}$	$C_{M\alpha}$
RMSE		0.1127	0.0141	0.0361
MAE		0.415	0.0781	0.1643
Forecast Delays s	η_{ice}=0.25	22.3199	2.8974	8.4664
	η_{ice}=0.5	17.7057	1.6608	9.4182

η_{ice}=0.75	10.6653	1.6171	7.5930
η_{ice}=0.95	5.2884	2.4171	8.1784

4. Icing Statistical Diagnosis Method

4.1 Generalized Likelihood Ratio Test

For the realistic problem, the probability density function (PDF) of a signal will be partly unknown due to some unknown parameters. The GLRT method estimates the unknown parameters by Maximum Likelihood estimators (MLEs) to solve these problems [26]. The detection problem can be mathematically expressed as:

$$\begin{aligned} &\mathcal{H}_0 : x[n] = w[n], \quad n = 0,1,\cdots,N-1 \\ &\mathcal{H}_1 : x[n] = A + w[n], \quad n = 0,1,\cdots,N-1 \end{aligned} \tag{11}$$

where x denotes the testing signal, A is unknown with $-\infty<A<\infty$ and $w[n]$ is white Gaussian noise with unknown variance σ^2. N is the window size. The $\mathcal{H}_0$ hypothesis describes the case where the unknown parameter A equals zero, whereas the alternative hypothesis $\mathcal{H}_1$ describes the case where the unknown parameter has an offset from zero. Meanwhile, the signal contains noise with unknown statistical characteristics in both hypotheses.

The GLRT can be used to distinguish between the two hypotheses. Based on the likelihood ratio between the probability of the two hypotheses, the test statistic for the problem in equation (11) decides $\mathcal{H}_1$ in a given window size of data if

$$L_G(x) = \frac{p\left(x;\hat{A},\hat{\sigma}_1^2,\mathcal{H}_1\right)}{p\left(x;\hat{\sigma}_0^2,\mathcal{H}_0\right)} > \gamma \tag{12}$$

where $\left(\hat{A},\hat{\sigma}_1^2\right)$ is the MLE of the parameters $\left(A,\sigma^2\right)$ under $\mathcal{H}_1$ and $\hat{\sigma}_0^2$ is the MLE of the parameter σ^2 under $\mathcal{H}_0$. γ denotes the threshold. With the MLEs the following test statistic can be derived and its asymptotic PDF is

$$T(x) = N\ln\left(1+\frac{\bar{x}^2}{\hat{\sigma}_1^2}\right) \sim \begin{cases} \chi_1^2 & \text{under } \mathcal{H}_0 \\ \chi_1^2(\lambda) & \text{under } \mathcal{H}_1 \end{cases} \tag{13}$$

where the MLE of the unknown parameters can be written as

$$\begin{aligned} &\hat{A} = \bar{x} \\ &\hat{\sigma}_1^2 = (1/N)\sum_{n=0}^{N-1}\left(x[n]-\bar{x}\right)^2 \end{aligned} \tag{14}$$

The noncentrality parameter $\lambda = NA^2/\sigma^2$. Then the threshold can be determined according to the NP theorem, that is for a given $P_{FA}=\alpha$, the threshold γ is found from equation (15) and maximizes the probability of detection P_D under $\mathcal{H}_1$.

$$P_{FA} = \int_{\{x:L_G(x)>\gamma\}} p\left(x;\mathcal{H}_0\right)dx \tag{15}$$

where $p(\cdot)$ is the probability distribution function of a given test statistic.

4.2 Residual Analysis

Ice accretion on the leading edge of wings changes the aircraft structure and causes the variation of the aerodynamic parameters. Although the ice accretion causes the obviously periodic vibration of the aircraft flight states, it doesn't mean the flight states are suitable for the statistical diagnosis. Because the state variables are the integral or multiple integral results of the changing aerodynamic parameters, which means the bias existing in state signals is not only related to the variation of the aerodynamic parameters, but also related to the noises and accumulative errors. Thus, the signal directly related to the changing aerodynamic parameters is needed for statistical diagnosis, such as the axial and normal overloads presented by Sorensen [24]. As same as the overloads, the angular accelerations are also directly affected by aerodynamic parameters, their changes indicate the changing of forces and moments. If the engine forces and moments are all known, the overloads and

angular accelerations are the perfect observing objects for ice detection. The estimation of overloads and angular accelerations is directly based on the dynamic equations, and for the problem in this paper, it can be calculated by equation (16).

$$\begin{aligned} N_x^{est} &= \frac{\left[-q_\infty S\left(C_D^{clean}\cos\alpha - C_L^{clean}\sin\alpha\right)+P_x\right]}{mg_0} \\ N_z^{est} &= \frac{\left[-q_\infty S\left(C_D^{clean}\sin\alpha + C_L^{clean}\cos\alpha\right)+P_z\right]}{mg_0} \\ \dot{q}^{est} &= \frac{q_\infty S b_A C_M^{clean} + M_y}{I_{yy}} \end{aligned} \tag{16}$$

where g_0 is the gravitational constant. If the ice accretion causes the aerodynamic coefficients displaying unexpected changes, a bias will be introduced into the residuals, and then the statistical diagnosis method can be used to detect the changes in the residual signals and trigger an icing alarm.

4.3 Diagnosis Algorithm Assessment

The same steady-level cruise scenario with wing ice in section 3.2 is utilized to assess the GLRT algorithm. Additionally, process and measurement noises are considered for assessing the performance of GLRT. We assume the process noises are independent vertical and horizontal acceleration perturbations. White Gaussian noise with the intensity of [0.1m/s, $0.1/V_0$]^T is used for both V and α, and the other flight statuses are assumed to have zero process noises. Addition to the variables in Table 4, the overloads measurement noises are given for using the diagnosis algorithm. The standard deviations of the two overloads are both set to 0.01g. The wing ice is assumed to occur at 200s, the ice accretion time T_{cld} and the two accretion rates are the same as the scenario in section 3.2.

The GLRT method is utilized to detect the aircraft wing ice and give an inflight icing alarm. The three generated residuals are used to monitor the icing situation. The residual data segments within a given window size are successively taken out for statistical diagnosis. When the test statistic exceeds the threshold, then the wing ice is detected.

The three residuals generated by the flight scenario are used to assess the performance of GLRT method. The trade-off between a high probability of detection P_D and a low probability of false alarm P_{FA} needs to be concerned for GLRT diagnosis. In this paper a small P_{FA} of 1e-6 is used, then the right-tail probability of χ_1^2 distribution under $\mathcal{H}_0$ is used to calculate the threshold. For this problem, the threshold is constant and equals 23.93. The influence of window size is discussed. Long-time intervals are not good for alarming timely. Here the window size between 1s to 40s and sampling frequency of 100Hz are chosen. The results of alarming time and probability of detection P_D under different window sizes by the three residuals are shown in Figure 4. The results indicate small window size will degrade the detection performance with the longer alarming time delay and the lower probability of detection. Detecting by the residual of N_x has the longer time delay than by the other two residuals. Diagnosing by the residual of N_z has higher probability of detection P_D than by the other two residuals. Increasing the window size reduces the alarming time to the range of [270, 290]s by the residuals of N_z and dq/dt. The results also show that diagnosing by residual N_z is more reliable than by the other two residuals, it is probably because the aircraft wing ice causes the more obvious normal offset.

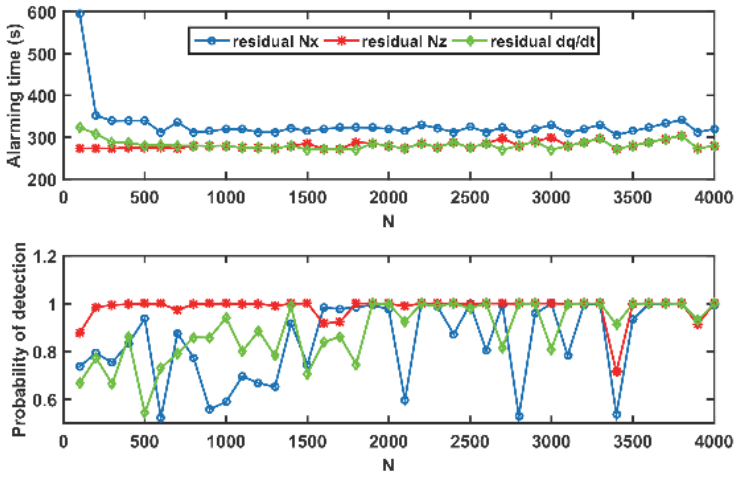

Figure 4 – Icing alarming time and probability of detection under different window sizes.

5. Inflight Icing Detection Strategy

An inflight icing detection strategy is proposed by combining the parameter identification method with the statistical diagnosis method to remedy their own defects. Figure 5 gives a scheme of combining the two methods for icing detection. First, the statistical diagnosis method is used to detect the changing of system outputs, if the obvious varying of output is detected then the wing ice is decided. The diagnosis method gives the ice occurring time and the disturbance signal is generated and superposed to the trimmed input signal to enhance the performance of the parameter identification method. Last, the time-varying aerodynamic parameters are identified by the disturbed system input and output. The problem of improving parameter inflight identifiability is resolved by this detection strategy. The capability of ice detection algorithm is augmented by this strategy of giving the icing occurring time and the changing information of aerodynamic parameters in one scheme.

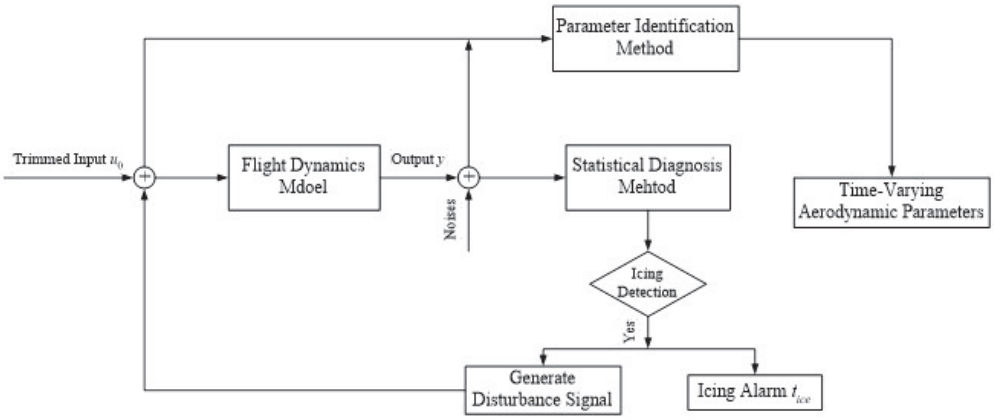

Figure 5 – A scheme of aircraft inflight icing detection.

The flight scenario presented above is utilized to assess this detection strategy. The flight time is 500s, wing ice occurs at 100s, the ice accretion time and the two accretion rates are the same as the scenario in section 3.2. Based on the conclusion in section 4.3, the normal overload N_z is chosen as the diagnosis signal, the window size of 5s (500 samples) is taken for GLRT method. Before the wing ice is detected by GLRT method, we recognize that the aerodynamic derivatives have not influenced by wing ice yet. If the icing alarm is triggered, the H∞ method is utilized to filter the output and identify the three stability derivatives. For the steady-level cruise scenario, the wing ice is found at 169.99s by the detection algorithm, the probability of detection P_D is 66.96% for a small P_{FA} of 1e-6. Meanwhile, the sixty “3211” disturbance signals each with amplitude of 5° and bandwidth of 5s successively added to the trimmed input. The three time-varying stability aerodynamic derivatives are identified by

H∞ method. Figure 6 shows the comparison of the identified results of three derivatives with their real values. Because of the oscillation of the identified result of $C_{D\alpha}$, the Y-axis of $C_{D\alpha}$ is shrunk to the range of [-0.5, 1.5] for better display. The results indicate the measurement noises seriously affect the identified result of $C_{D\alpha}$ and cause a wide range oscillation after the wing ice is detected, but the identified results of $C_{L\alpha}$ and $C_{M\alpha}$ are barely influenced by the noises. Even with the measurement noises, the three derivatives all converge to their real values. Although the alarming time delay (about 70s for this scenario) of the statistical diagnosis method is difficult to eliminate, the high accuracy of $C_{L\alpha}$ and $C_{M\alpha}$ results validates the effectiveness of the detection algorithm.

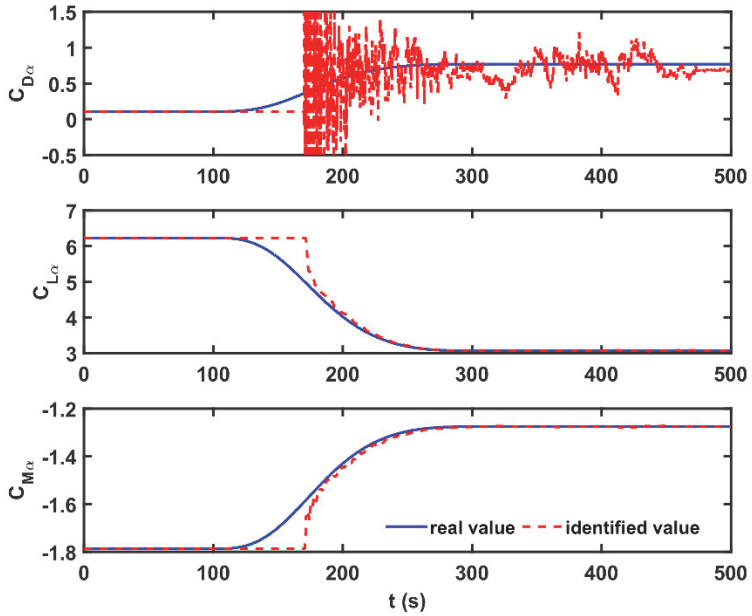

Figure 6 – Aerodynamic stability derivates identified by ice detection strategy.

6. Conclusion

The aircraft inflight icing detection methods are discussed in this paper. First, the time-varying parameter identification method and statistical diagnosis method are presented respectively. The aircraft inflight icing dynamics is modelled for an icing research airbus with ice accreting on the leading edge of wings. The simulation data based on the dynamic model is used to verify performance of the two methods. Based on the researches, a strategy of combining these two methods is proposed to monitor the ice occurring time and identify the time-varying aerodynamic derivatives. The flight scenario of the icing research airbus is utilized to assess this strategy. The results indicate the wing ice can be detected by the diagnosis method and the three stability derivatives can be identified in a relatively high accuracy by superposing a small disturbance signal to the trimmed input. The research in this paper preliminarily demonstrates the feasibility of the inflight icing detection strategy. The combination of different icing detection methods enhances the capability of the single method and will expand the application of ice detection by algorithm technique in aviation industry.

The future research on aircraft inflight icing detection needs to focus on the further application of the algorithm detection method in real flight tests. For doing that, there are several points need to be issued, such as the inevitable time delay of statistical decision theory-based methods normally reaches tens or hundreds of seconds; the identifiability and accuracy of parameter estimation method seriously depends on the excited system dynamic characteristics; the difficulty in detecting the ice accretion finish time might influence the identifiability of the time-varying aerodynamic parameters because of the uncertainty of the time coverage of the disturbance signal; the mechanism of noises

affecting the accuracy of parameter identification results is also needed to be recognized in the future work.

7. Archiving

The research was sponsored by the National Natural Science Foundation of China (NSFC) under grant No. 11802325.

8. Contact Author Email Address

Dr. Di Ding

Mailto: dingdi1981@cardc.cn

9. Copyright Statement

References

[1] Cao Y H, Wu Z L, Su Y and Xu Z D. Aircraft flight characteristics in icing conditions. *Progress in Aerospace Sciences*, vol. 74, pp 62–80, Apr. 2015.

[2] Goraj Z. An overview of the de-icing and anti-icing technologies with prospects for the future. *24th International Congress of Aeronautical Sciences*, Japan Yokohama, Paper ICAS 2004-7.5.1 (I.L.), 2004.

[3] Jarvinen P. Aircraft ice detection method. *45th AIAA Aerospace Sciences Meeting and Exhibit*, Reno NV, Paper AIAA-2007-696, 2007.

[4] Bragg M B, Basar T and Perkins W R. Smart icing systems for aircraft icing safety. *40th AIAA Aerospace Sciences Meeting and Exhibit*, Reno NV, Paper AIAA-2002-0813, 2002.

[5] Wenz A and Johansen T A. Icing detection for small fixed wing UAVs using inflight aerodynamic coefficient estimation. *2016 IEEE Conf. on Control Applications,* Buenos Aires, pp 230-236, 2016.

[6] Melody J W, Basar T and Perkins W R. Parameter identification for inflight detection and characterization of aircraft icing. *Control Engineering Practice,* Vol. 8, No. 9, pp 985-1001, Sep. 2000.

[7] Melody J W, Hillbrand T and Basar T. H_∞ parameter identification for inflight detection of aircraft icing: The time-varying case. *Control Engineering Practice,* Vol. 9, No. 12, pp 1327-1335, Dec. 2001.

[8] Melody J W. *Inflight characterization of aircraft icing*. Ph.D. dissertation, Dept. Elect. Eng., Univ. of Illinois at Urbana-Champaign, 2004.

[9] Cristofaro A, Johansen T A and Aguiar A P. Icing detection and identification for Unmanned Aerial Vehicles: Multiple Model Adaptive Estimation. *2015 European Control Conf.,* Linz, pp 1651-1656, 2015.

[10] Cristofaro A, Johansen T A and Aguiar A P. Icing detection and identification for unmanned aerial vehicles using adaptive nested multiple models. *International Journal of Adaptive Control and Signal Processing*, Vol. 31, No. 11, pp 1584-1607, Nov. 2017.

[11] Ying S B, Ge T and Ai J L. H_∞ parameter identification and H_2 feedback control synthesizing for inflight aircraft icing. *J. Shanghai Jiaotong Univ (Sci),* Vol. 18, No. 3, pp 317-325, 2013.

[12] Caliskan F, Aykan R and Hajiyev C. Aircraft icing detection, identification, and reconfigurable control based on kalman filtering and neural networks. *Journal of Aerospace Engineering,* Vol. 21, No. 2, pp 51–60, 2008.

[13] Caliskan F. Neural network based icing identification and fault tolerant control of a 340 aircraft. *International Journal of Electrical, Computer, and Systems Engineering,* Vol. 1, No. 2, pp 98–103, 2007.

[14]Schuchard E A, Melody J W and Basar T. Detection and classification of aircraft icing using Neural Networks. 38th *Aerospace Sciences Meeting and Exhibit*, Reno NV, Paper AIAA-2000-0361, 2000.

[15]Dong Y Q and Ai J L. Research on inflight parameter identification and icing location detection of the aircraft. *Aerospace Science and Technology,* Vol. 29, No. 1, pp 305-312, Aug. 2013.

[16]Dong Y Q and Ai J L. Inflight parameter identification and icing location detection of the aircraft: The time-varying case. *Journal of Control Science and Engineering,* Vol. 2014, pp 1-11, 2014.

[17]Shen Q K, Jiang B and Cocquempot V. Adaptive fault-tolerant backstepping control against actuator gain faults and its applications to an aircraft longitudinal motion dynamics. *International Journal of Robust and Nonlinear Control*, Vol. 23, No. 15, pp 1753-1779, 2013.

[18]Shen Q K, Jiang B and Shi P. Adaptive fault diagnosis for T-S fuzzy systems with sensor faults and system performance analysis. *IEEE Trans. On Fuzzy Systems*, Vol. 22, No. 2, pp 274-285, 2014.

[19]Miller R H and Ribbens W B. Detection of the loss of elevator effectiveness due to aircraft icing. *37th Aerospace Sciences Meeting and Exhibit*, Reno NV, Paper AIAA-99-0637, 1999.

[20]Tousi M M and Khorasani K. Fault diagnosis and recovery from structural failures (icing) in unmanned aerial vehicles. *IEEE SysCon 2009,* Vancouver, pp 302–307, 2009.

[21]Tousi M M and Khorasani K. Robust observer-based fault diagnosis for an unmanned aerial vehicle. *IEEE Int. SysCon 2011,* Montreal, pp 428–434, 2011.

[22]Caliskan F and Hajiyev C. A review of in-flight detection and identification of aircraft icing and reconfigurable control. *Progress in Aerospace Sciences*, Vol. 60, pp 12–34, 2013.

[23]Mehra R K and Peschon J. An innovations approach to fault detection and diagnosis in dynamic systems. *Automatica*, Vol. 7, No. 5, pp 637-640, 1971.

[24]Sorensen K L, Blanke M and Johansen T A. Diagnosis of wing icing through lift and drag coefficient change detection for small unmanned aircraft. *IFAC-PapersOnLine*, Vol. 48, No. 21, pp 541-546, 2015.

[25]DIDINSKY G, PAN Z and BASAR T. Parameter identification for uncertain plants using H_∞ methods. *Automatica*, Vol. 31, No. 9, pp 1227-1250, 1995.

[26]Kay S M. *Fundamentals of Statistical Signal Processing: Detection Theory*. USA: Prentice Hall PTR, pp 341–349, 1998.